Structural Engineering and Mechanics, *Vol. 66, No. 3 (2018) 317-328*
DOI: https://doi.org/10.12989/sem.2018.66.3.317

Analytical investigation of bending response of FGM plate using a new quasi 3D shear deformation theory: Effect of the micromechanical models

Rabbab Bachir Bouiadjra[*1], Abdelkader Mahmoudi[2a], Samir Benyoucef[2b], Abdelouahed Tounsi[2,3c] and Fabrice Bernard[4d]

[1]*Department of Civil Engineering, University Mustapha Stambouli of Mascara, Algeria*
[2]*Department of Civil Engineering, Material and Hydrology Laboratory, University of Sidi Bel Abbes, Faculty of Technology, Algeria*
[3]*Department of Civil and Environmental Engineering, King Fahd University of Petroleum & Minerals, 31261 Dhahran, Eastern Province, Saudi Arabia*
[4]*Laboratoire de Génie Civil et Génie Mécanique, INSA de Rennes, France*

(Received August 6, 2017, Revised January 22, 2018, Accepted February 27, 2018)

Abstract. In this paper, a new refined quasi-three-dimensional (3D) shear deformation theory for the bending analysis of functionally graded plate is presented. The number of unknown functions involved in this theory is only four against five or more in the case of the other shear and normal deformation theories. Due to its quasi-3D nature, the stretching effect is taken into account in the formulation of governing equations. In addition, the effect of different micromechanical models on the bending response of these plates is studied. Various micromechanical models are used to evaluate the mechanical characteristics of the FG plates whose properties vary continuously across the thickness according to a simple power law. The present theory accounts for both shear deformation and thickness stretching effects by a parabolic variation of displacements across the thickness, and the zero traction boundary conditions on the top and bottom surfaces of the plate without using shear correction factors. The problem is solved for a plate simply supported on its edges and the Navier solution is used. The results of the present method are compared with others from the literature where a good agreement has been found. A detailed parametric study is presented to show the effect of different micromechanical models on the flexural response of a simply supported FG plates.

Keywords: FG plates; micromechanical models; quasi 3D shear deformation theory; stretching effect; bending

1. Introduction

Normally, the interest of researches in functionally graded materials (FGMs) has intensified considerably since their first introduction in mid-1980s by Japanese material scientists (Koizumi 1993).

The FGMs are part of a relatively new trend in materials science. They are advanced composite materials with gradual and continuous variation in the volume fractions of each constituent, generating changes in the properties of the materials, eliminating discontinuities at the interfaces, while the characteristics of the constituent materials are preserved. They can thus combine the properties of the two totally different constituents without one making concessions for the benefit of the other. This new class of materials has attracted particular attention and interest in the last three decades. Their use is increasing in the aeronautics, aerospace, civil engineering and many other sectors where they can serve as thermal barriers to their rich ceramic composition. From the above, it is therefore necessary to develop accurate theories to describe and understand the behavior of the structures made from these materials.

Several FGM plate analysis were performed according to the classical plate theory (CPT), first-order shear deformation theory (FSDT) and higher order plate theory (HSDT).

The most fundamental deformation theory is classical plate theory (CPT), the latter does not give precise results in the case of thick or relatively thick plates because it neglects the effects of shear deformation. On the other hand in the case of thin plates, it gives more or less precise results.

Using CPT, Chi and Chung (2006a, 2006b) have developed analytical solution for simply supported FG plates subjected to mechanical loads. Chi and Chung (2006) presented an analytical formulation for simply supported rectangular FG plates subjected to transverse loading. Three different distribution of the volume fraction across the thickness were used.

The FSDT was developed to overcome the limitation of the CPT. It gives acceptable results for moderately thick plates. On the other hand, it requires the introduction of a shear correction factor due to its violation the equilibrium conditions at the top and bottom surfaces of the plate. This factor corrects the unrealistic variation of transverse shear stresses and shear strain through the thickness (Fekrar *et al.* 2014). Bellifa *et al.* (2016) have presented a new first-order shear deformation theory for bending and dynamic

∗Corresponding author, Ph.D.
E-mail: bbrabab@gmail.com
[a]Student
[b]Professor
[c]Ph.D.

ISSN: 1225-4568 (Print), 1598-6217 (Online)

behaviors of functionally graded plates. The number of unknowns is the least one comparing with the traditional first-order shear deformation theories. Ouled youcef *et al.* (2018) have developed an analytic non-classical model for the free vibrations of nano beams accounting for surface stress effects.

In order to avoid the use of a shear correction factor, several Higher order Shear Deformation Theories (HSDT) have been developed and proposed. The HSDT theories can be developed in two ways: polynomial or non-polynomial. In the polynomial case, the effects of shear deformations are taken into account using a Taylor series development (Gupta and Talha 2017). These theories are laborious because they contain several unknowns (Gupta and Talha 2017). For example, Reddy (2000) have developed a theory with seven unknowns and Talha and Singh (2010, 2011) with thirteen.

In the case of the non-polynomial shear deformation theory, the number of unknowns is lower than the previous ones. We can cite as an example, Akavci (2014) present a five unknowns hyperbolic function and Neves *et al.* (2012) who proposed a hyperbolic theory with six unknowns.

Also, many papers are published concerning with analysis of FGM structures based on HSDTs (see Bourada *et al.* 2012, Bousahla *et al.* 2014, Bennoun *et al.* 2016, Bellifa *et al.* 2016, Ait atmane *et al.* 2015, Bourada *et al.* 2015 and Merazi *et al.* 2015). Recently, Tounsi and his co-workers (Hadji *et al.* 2011, Houari *et al.* 2011, Abdelaziz *et al.* 2011, Merdaci *et al.* 2011, Bouderba *et al.* 2013 and Taibi *et al.* 2015, Ait Amar Meziane *et al.* (2014)) have developed a new four variable refined plate theory which involves only four unknown function for bending response, thermo-mechanical bending response, buckling and free vibration of simply supported FGM sandwich plate. Boukhari *et al.* (2016) have used the same theory to analyze the wave propagation of an infinite functionally graded plate in the presence of thermal environments. Using a new displacement field which includes undetermined integral variables, Bellifa *et al.* (2017) have proposed a simple refined theory for buckling analysis of functionally graded plates. Furthermore, Tounsi *et al.* (2016) presented a new 3-unknowns non-polynomial plate theory for buckling and vibration of FG sandwich plate. Houari *et al.* (2016) have used the same theory to study the bending and free vibration analysis of functionally graded (FG) plates.

One of the key assumptions of FSDT and HSDT is that the transverse displacement through the thickness of the plate is constant. This led to neglect the thickness stretching. However, this assumption is inadequate for thick FGM plates.

To remedy this problem and in order to take into account the effects of the deformations due to the stretching, theories called Quasi-3D have appeared. These theories are HSDTs in which the transverse displacement is expressed as a high order variation through the thickness of the plate, and hence, thickness-stretching effect is captured (Huu-Tai *et al.* 2014).

Using a Quasi-3D shear deformation theory, Farzam-Rad *et al.* (2016) have studied the bending response of FGM plate with five unknowns. The static and free vibration analysis of the FG plates was studied by Hebali *et al.* (2014) using theory with the same numbers of unknowns. Bessaim *et al.* (2013) have presented a new higher-order shear and normal deformation theory for the bending and free vibration analysis of sandwich plates with FG face sheets. Based on a layer-wise approach, Brischetto (2014) has developed a 3-D solution for free vibration of multilayered and sandwich plates and shells. Abualnour *et al.* (2018) have developed a new shear deformation theory including the stretching effect for free vibration of the simply supported functionally graded plates. Draiche *et al.* (2016) have presented a refined theory with stretching effect for static flexure analysis of laminated composite plates. Benchohra *et al.* (2018) proposed a new quasi-3D sinusoidal shear deformation theory for functionally graded (FG) plates.

In order to model FGM precisely, it is essential to know the effective or bulk material properties as a function of individual material properties and geometry, in particular at micromechanics level.

In recent years, different models have been proposed to estimate the effective properties of FGMs with respect to reinforcement volume fractions (Shen HS and Wang ZX (2012), Jha DK *et al.* (2013)). Consequently, several micromechanical models have been used to study and analyze the behavior of FGM structures under different loading conditions. We cite as an example the work of Gasik (1998) in which he proposed a micromechanical model to study FGMs with a random distribution of constituents. The FGM microstructures were idealized by homogeneous materials (sub-cells) with cubic inclusions. Each substring corresponded to a fixed volume. Thereafter, the elastic constants as well as the coefficient of thermal expansion calculated from its model were compared with those obtained from the Mori-Tanaka Voigt, and Kerner's models.

The effective linear thermal conductivity and linear elastic constants of FGM fiber reinforced composites have been determined by Ostoja-Starzewski *et al.* (1996) by means of a micromechanical model.

Using an appropriate micromechanical model, Yin *et al.* (2004) and Yin *et al.* (2007) have determined the expressions of the linear coefficient of thermal expansion, the Young's moduli and the Poisson's ratio.

The heat conduction and the thermo-elastic deformations of the FGM have been studied by Aboudi *et al.* (1996, 1999) and Pindera *et al.* (2002) from the higher order micromechanical models based on the method of cells. The FGMs studied had one, two, and three graded directions.

This study presents a micromechanical model for predicting the bending response of FGM plate. A new quasi-3D shear deformation theory with only four unknowns and thickness-stretching effect is presented. The number of unknowns of the present theory is only four which less than the other shear and normal deformation theories where we find five, six or more variables. Micromechanical models are used to determine through-thickness the effective material properties of FGMs with power-law function distributions of volume fraction of a simply supported FG plates. Using an analytical method, the governing equations are treated and the effects of Voigt, Reuss, LRVE, Tamura and Mori-Tanaka models on deflection and stress of the FG plate are investigated.

2. Effective properties of FGMs

Unlike traditional microstructures, in FGMs the material properties are spatially varying, which is not trivial for a micromechanics model (Jaesang and Addis 2014).

A number of micromechanics models have been proposed for the determination of effective properties of FGMs. In what follows, we present some micromechanical models to calculate the effective properties of the FG plate.

2.1 Voigt model

The Voigt model is relatively simple; this model is frequently used in most FGM analyses estimates Young's modulus E of FGMs as (Mishnaevsky 2007, Zimmerman 1994)

$$E(z) = E_c\, V_c + E_m(1 - V_c) \tag{1}$$

2.2 Reuss model

Reuss assumed the stress uniformity through the material and obtained the effective properties as (Mishnaevsky 2007, Zimmerman 1994)

$$E(z) = \frac{E_c\, E_m}{E_c\,(1 - V_c) + E_m V_c} \tag{2}$$

2.3 Tamura model

The Tamura model uses actually a linear rule of mixtures, introducing one empirical fitting parameter known as "stress-to-strain transfer" (Gasik 1995, Zuiker 1995)

$$q = \frac{\sigma_1 - \sigma_2}{\varepsilon_1 - \varepsilon_2} \tag{3}$$

Estimate for q=0 correspond to Reuss rule and with q=100 to the Voigt rule, being invariant to the consideration of with phase is matrix and which is particulate. The effective Young's modulus is found as

$$E(z) = \frac{(1 - V_c)\, E_m\,(q - E_c) + V_c\, E_c\,(q - E_m)}{(1 - V_c)(q - E_c) + V_c\, E_c\,(q - E_m)} \tag{4}$$

2.4 Description by a representative volume element (LRVE)

The local representative volume element (LRVE) is based on a "mesoscopic" length scale which is much larger than the characteristic length scale of particles (inhomogeneities) but smaller than the characteristic length scale of a macroscopic specimen (Ju and Chen 1994). The LRVE is developed based on the assumption that the microstructure of the heterogeneous material is known. The input for the LRVE for the deterministic micromechanical framework is usually volume average or ensemble average of the descriptors of the microstructures.

Young's modulus is expressed as follows by the LRVE method (Akbarzadeh *et al.* 2015)

$$E(z) = E_m\left(1 + \frac{V_c}{FE - \sqrt[3]{V_c}}\right), \quad FE = \frac{1}{1 - \dfrac{E_m}{E_c}} \tag{5}$$

2.5 Mori-Tanaka model

The locally effective material properties can be provided by micromechanical models such as the Mori–Tanaka estimates. This method based on the assumption that a two-phase composite material consisting of matrix reinforced by spherical particles, randomly distributed in the plate. According to Mori-Tanaka homogenization scheme, the effective Bulk Modulus (K) and the effective shear modulus (G) are given by (Mori and Tanaka 1973, Benveniste 1987)

$$\begin{aligned} K(z) &= K_m + \frac{V_c\,(K_c - K_m)}{1 + (1 - V_c)3(K_c - K_m)/(3K_m + 4K_c)} \\ G(z) &= G_m + \frac{V_c\,(G_c - G_m)}{1 + (1 - V_c)(G_c - G_m)/(G_m + f_1)} \end{aligned} \tag{6a}$$

And

$$f_1 = \frac{G_m(9K_m + 8G_m)}{6(K_m + 2G_m)} \tag{6b}$$

The overall modulus of elasticity

$$E(z) = \frac{9K(z)G(z)}{3K(z) + G(z)} \tag{6c}$$

The effective Young's modulus (E) in terms of constituents is given by (Belabed *et al.* 2014, Abualnour *et al.* 2018)

$$E(z) = E_m + (E_c - E_m)\left(\frac{V_c}{1 + (1 - V_c)(E_c/E_m - 1)(1 + \upsilon)/(3 - 3\upsilon)}\right) \tag{6d}$$

In all models outlined above, E_i, V_i (i=c,m) are the Young's modulus and the volume fraction of the phase material respectively. The subscripts c and m refer to the ceramic and metal respectively. The volume fractions of the ceramic and metal phases are related by $V_c+V_m=1$, and V_c is expressed as

$$V_c = \left(0{,}5 + \frac{z}{h}\right)^p, \quad p \geq 0 \tag{7}$$

The effective mass density ρ is given by the rule mixtures as (See Bessaim *et al.* 2013, Benachour *et al.* 2011, Yaghoubi and Torabi 2013, Tounsi *et al.* 2013, Ould Larbi *et al.* 2013), regardless of the utilized micromechanical models

$$\rho = \rho_c\, V_c + \rho_m\, V_m \tag{8}$$

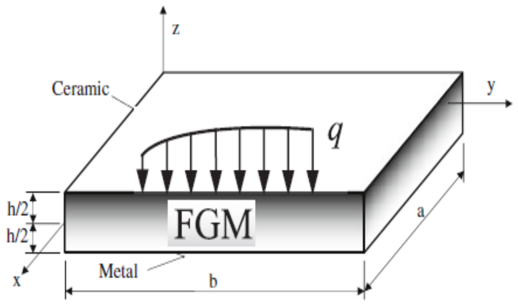

Fig. 1 Geometry of rectangular FG plate and coordinates

3. Kinematics

Consider a rectangular FG plate, with total thickness h, length a, and width b, referred to the rectangular Cartesian coordinates (x, y, z), as shown in Fig. 1. The plate is subjected to a transverse distributed load q(x,y).

The displacement field satisfying the conditions of transverse shear stresses (and hence strains) vanishing at (x, y, ±h/2) on thes outer (top) and inner (bottom) surfaces of the plate, is given as follows

$$\begin{aligned} u\ (x,y,z,t) &= u_0 - z\frac{\partial w_b}{\partial x} + f(z)\frac{\partial w_s}{\partial x} \\ v\ (x,y,z,t) &= v_0 - z\frac{\partial w_b}{\partial y} + f(z)\frac{\partial w_s}{\partial y} \\ w(x,y,z,t) &= w_b + g(z)w_s \end{aligned} \tag{9}$$

With

$$f(z) = z\left(1-\frac{4z^2}{3h^2}\right) \quad , \quad g(z) = \frac{1}{12}\frac{\partial f(z)}{\partial z} \tag{10}$$

Where $u_0(x,y)$, $v_0(x,y)$, $w_b(x,y)$ *and* $w_s(x,y)$ are the four unknown displacement functions of the middle surface of the plate.

The kinematic relations can be obtained as follows

$$\begin{aligned} &\begin{Bmatrix} \varepsilon_x \\ \varepsilon_y \\ \gamma_{xy} \end{Bmatrix} = \begin{Bmatrix} \varepsilon_x^0 \\ \varepsilon_y^0 \\ \gamma_{xy}^0 \end{Bmatrix} + z\begin{Bmatrix} k_x \\ k_y \\ k_{xy} \end{Bmatrix} + f(z)\begin{Bmatrix} \eta_x \\ \eta_y \\ \eta_{xy} \end{Bmatrix}, \varepsilon_z = g'(z)\varepsilon_z^0, \\ &\begin{Bmatrix} \gamma_{yz} \\ \gamma_{xz} \end{Bmatrix} = f'(z)\begin{Bmatrix} \gamma_{yz}^0 \\ \gamma_{xz}^0 \end{Bmatrix} + g(z)\begin{Bmatrix} \gamma_{yz}^0 \\ \gamma_{xz}^0 \end{Bmatrix} \end{aligned} \tag{11}$$

where

$$\begin{aligned} &\begin{Bmatrix} \varepsilon_x^0 \\ \varepsilon_y^0 \\ \gamma_{xy}^0 \end{Bmatrix} = \begin{Bmatrix} \dfrac{\partial u_0}{\partial x} \\ \dfrac{\partial v_0}{\partial y} \\ \dfrac{\partial u_0}{\partial y} + \dfrac{\partial v_0}{\partial x} \end{Bmatrix}, \begin{Bmatrix} k_x \\ k_y \\ k_{xy} \end{Bmatrix} = \begin{Bmatrix} -\dfrac{\partial^2 w_b}{\partial x^2} \\ -\dfrac{\partial^2 w_b}{\partial y^2} \\ -2\dfrac{\partial^2 w_b}{\partial x \partial y} \end{Bmatrix}, \\ &\begin{Bmatrix} \eta_x \\ \eta_y \\ \eta_{xy} \end{Bmatrix} = \begin{Bmatrix} \dfrac{\partial^2 w_s}{\partial x^2} \\ \dfrac{\partial^2 w_s}{\partial y^2} \\ 2\dfrac{\partial^2 w_s}{\partial x \partial y} \end{Bmatrix}, \begin{Bmatrix} \gamma_{yz}^0 \\ \gamma_{xz}^0 \end{Bmatrix} = \begin{Bmatrix} \dfrac{\partial w_s}{\partial y} \\ \dfrac{\partial w_s}{\partial x} \end{Bmatrix}, \varepsilon_z^0 = w_s \end{aligned} \tag{12}$$

4. Constitutive relations

The linear constitutive relations are

$$\begin{pmatrix} \sigma_x \\ \sigma_y \\ \sigma_z \\ \tau_{yz} \\ \tau_{xz} \\ \tau_{xy} \end{pmatrix} = \begin{bmatrix} Q_{11} & Q_{12} & Q_{13} & 0 & 0 & 0 \\ Q_{12} & Q_{22} & Q_{23} & 0 & 0 & 0 \\ Q_{13} & Q_{23} & Q_{33} & 0 & 0 & 0 \\ 0 & 0 & 0 & Q_{44} & 0 & 0 \\ 0 & 0 & 0 & 0 & Q_{55} & 0 \\ 0 & 0 & 0 & 0 & 0 & Q_{66} \end{bmatrix} \begin{pmatrix} \varepsilon_x \\ \varepsilon_y \\ \varepsilon_z \\ \gamma_{yz} \\ \gamma_{xz} \\ \gamma_{xy} \end{pmatrix} \tag{13}$$

where (σ_x, σ_y, σ_z, τ_{xy}, τ_{yz}, τ_{yx}) and (ε_x, ε_y, ε_z, γ_{xy}, γ_{yz}, γ_{yx}) are the stress and strain components, respectively. Using the material properties defined above, stiffness coefficients, Q_{ij} can be expressed as

$$\begin{aligned} Q_{11} = Q_{22} = Q_{33} &= \frac{E(z)(1-\nu)}{(1-2\nu)(1+\nu)} \quad , \\ Q_{12} = Q_{13} = Q_{23} &= \frac{\nu E(z)}{(1-2\nu)(1+\nu)} \quad , \\ Q_{44} = Q_{55} = Q_{66} &= \frac{E(z)}{2(1+\nu)} \end{aligned} \tag{14}$$

5. Equations of motion

Considering the static version of the principle of virtual work, the following expressions can be obtained

$$\begin{aligned} &\int_\Omega \int (\sigma_x\,\delta\varepsilon_x + \sigma_y\,\delta\varepsilon_y + \sigma_z\,\delta\varepsilon_z + \tau_{xy}\,\delta\gamma_{xy} \\ &\quad + \tau_{xz}\,\delta\gamma_{xz} + \tau_{yz}\,\delta\gamma_{yz})d\Omega\,dz - \int_\Omega q\delta w d\Omega = 0 \end{aligned} \tag{15}$$

Where Ω is the top surface, q is the distributed transverse load.

Substituting Eqs. (11) and (13) into Eq. (15) and integrating through the thickness of the plate, we can obtain

$$\begin{aligned} &\int_\Omega \{ N_1\delta\varepsilon_x^0 + M_1\,\delta k_x + P_1\delta\eta_x + N_2\delta\varepsilon_y^0 + M_2\,\delta k_y + P_2\delta\eta_y \\ &\quad + R_3\delta\varepsilon_z^0 + Q_4\delta\gamma_{yz}^0 + K_4\delta\gamma_{yz}^0 + Q_5\delta\gamma_{xz}^0 + K_5\delta\gamma_{xz}^0 \\ &\quad + N_6\delta\gamma_{xy}^0 + M_6\delta k_{xy} + P_6\delta\eta_{xy} \} d\Omega - \int_\Omega q\delta w d\Omega = 0 \end{aligned} \tag{16}$$

The stress resultants N, M, P, Q and R are defined by

$$\begin{aligned} (N_i, M_i, P_i) &= \int_{-h/2}^{h/2} \sigma_i\,(1, z, f(z))dz, \qquad (i = 1,2,6) \\ (K_i, Q_i) &= \int_{-h/2}^{h/2} \sigma_i\left(f'(z), g(z)\right)dz, \qquad (i = 4,5) \\ R_i &= \int_{-h/2}^{h/2} \sigma_i g'(z)dz, \qquad (i = 3) \end{aligned} \tag{17}$$

The governing equations of equilibrium can be derived from eq. (16) by integrating the displacement gradients by parts and setting the coefficients where δu_0, $\delta v_0, \delta w_b$, δw_s zero.

Thus, one can obtain the equilibrium equations associated with the present shear deformation theory

$$\begin{aligned}
&\delta u_0 : \frac{\partial N_1}{\partial x} + \frac{\partial N_6}{\partial y} = 0 \\
&\delta v_0 : \frac{\partial N_6}{\partial x} + \frac{\partial N_2}{\partial y} = 0 \\
&\delta w_b : \frac{\partial^2 M_1}{\partial x^2} + 2\frac{\partial^2 M_6}{\partial x \partial y} + \frac{\partial^2 M_2}{\partial y^2} = -q \\
&\delta w_s : -\frac{\partial^2 P_1}{\partial x^2} - \frac{\partial^2 P_2}{\partial y^2} - 2\frac{\partial^2 P_6}{\partial x \partial y} + \frac{\partial Q_4}{\partial y} + \frac{\partial K_4}{\partial y} \\
&\qquad + \frac{\partial Q_5}{\partial x} + \frac{\partial K_5}{\partial x} - R_3 = -g(z)\, q
\end{aligned} \tag{18}$$

Using Eq. (13) in Eq. (17), the stress resultants of the sandwich plate can be related to the total strains by

$$\begin{aligned}
N_i &= A_{ij}\varepsilon_j^0 + B_{ij}k_j + C_{ij}\eta_j + F_{ij}\varepsilon_z^0, && (i=1,2,6) \\
M_i &= B_{ij}\varepsilon_j^0 + G_{ij}k_j + H_{ij}\eta_j + K_{ij}^{'}\varepsilon_z^0, && (i=1,2,6) \\
P_i &= C_{ij}\varepsilon_j^0 + H_{ij}k_j + L_{ij}\eta_j + O_{ij}\varepsilon_z^0, && (i=1,2,6) \\
Q_i &= Q_{ij}^{'}\gamma_j^0 + P_{ij}^{'}\gamma_j^0, && (i=4,5) \\
K_i &= Q_{ij}^{'}\gamma_j^0 + S_{ij}\gamma_j^0, && (i=4,5) \\
R_i &= F_{ij}\varepsilon_j^0 + K_{ij}^{'}k_j + O_{ij}\eta_j + U_{ij}\varepsilon_z^0, && (i=3)
\end{aligned} \tag{19}$$

Where

$$\begin{aligned}
&\left(A_{ij}, B_{ij}, C_{ij}, D_{ij}, E_{ij}, F_{ij}\right) = \int_{-h/2}^{h/2} Q_{ij}\left(1, z, f(z),\ g(z),\ f^{'}(z), g^{'}(z)\right)dz \\
&\left(G_{ij}, H_{ij}, K_{ij}^{'}, L_{ij}\right) = \int_{-h/2}^{h/2} Q_{ij}\left(z^2, zf(z), zg^{'}(z),\ f^2(z)\right)dz \\
&\left(O_{ij}, P_{ij}^{'}, Q_{ij}^{'}, S_{ij}\right) = \int_{-h/2}^{h/2} Q_{ij}\left(f(z)g^{'}(z),\ g^2(z), g(z)f^{'}(z),\ f^{'2}(z)\right)dz \\
&U_{ij} = \int_{-h/2}^{h/2} Q_{ij}\left(g^{'2}(z)\right)dz
\end{aligned} \tag{20}$$

By substituting Eqs. (19) into Eqs. (18), the equilibrium equations can be expressed in terms of displacements $\left(u_0, v_0, w_b, w_s\right)$ as

$$\begin{aligned}
&A_{11}\frac{\partial^2 u_0}{\partial x^2} + A_{66}\frac{\partial^2 u_0}{\partial y^2} + (A_{12}+A_{66})\frac{\partial^2 v_0}{\partial x \partial y} - B_{11}\frac{\partial^3 w_b}{\partial x^3} + C_{11}\frac{\partial^3 w_s}{\partial x^3} \\
&-(B_{12}+2B_{66})\frac{\partial^3 w_b}{\partial x \partial y^2} + (C_{12}+2C_{66})\frac{\partial^3 w_s}{\partial x \partial y^2} + F_{12}\frac{\partial w_s}{\partial x} = 0 \\
&A_{22}\frac{\partial^2 v_0}{\partial y^2} + A_{66}\frac{\partial^2 v_0}{\partial x^2} + (A_{12}+A_{66})\frac{\partial^2 u_0}{\partial x \partial y} - B_{22}\frac{\partial^3 w_b}{\partial y^3} + C_{22}\frac{\partial^3 w_s}{\partial y^3} \\
&-(B_{12}+2B_{66})\frac{\partial^3 w_b}{\partial x^2 \partial y} + (C_{12}+2C_{66})\frac{\partial^3 w_s}{\partial x^2 \partial y} + F_{23}\frac{\partial w_s}{\partial y} = 0 \\
&B_{11}\frac{\partial^3 u_0}{\partial x^3} + (B_{12}+2B_{66})\left(\frac{\partial^3 u_0}{\partial x \partial y^2} + \frac{\partial^3 v_0}{\partial x^2 \partial y}\right) + B_{22}\frac{\partial^3 v_0}{\partial y^3} - G_{11}\frac{\partial^4 w_b}{\partial x^4} \\
&-2(G_{12}+2G_{66})\frac{\partial^4 w_b}{\partial x^2 \partial y^2} - G_{22}\frac{\partial^4 w_b}{\partial y^4} + H_{11}\frac{\partial^4 w_s}{\partial x^4} + H_{22}\frac{\partial^4 w_s}{\partial y^4} \\
&+2(H_{12}+2H_{66})\frac{\partial^4 w_s}{\partial x^2 \partial y^2} = -q \\
&-C_{11}\frac{\partial^3 u_0}{\partial x^3} - (C_{12}+2C_{66})\frac{\partial^3 u_0}{\partial x \partial y^2} - (C_{12}+2C_{66})\frac{\partial^3 v_0}{\partial x^2 \partial y} - C_{22}\frac{\partial^3 v_0}{\partial y^3} \\
&-F_{13}\frac{\partial u_0}{\partial x} - F_{23}\frac{\partial v_0}{\partial y} + H_{11}\frac{\partial^4 w_b}{\partial x^4} + H_{22}\frac{\partial^4 w_b}{\partial y^4} + 2(H_{12}+2H_{66})\frac{\partial^4 w_b}{\partial x^2 \partial y^2} \\
&+K_{13}^{'}\frac{\partial^2 w_b}{\partial x^2} + K_{23}^{'}\frac{\partial^2 w_b}{\partial y^2} - L_{11}\frac{\partial^4 w_s}{\partial x^4} - 2(L_{12}+2L_{66})\frac{\partial^4 w_s}{\partial x^2 \partial y^2} - L_{22}\frac{\partial^4 w_s}{\partial y^4} \\
&+(P_{55}^{'}+2Q_{55}^{'}-2O_{13}+S_{55})\frac{\partial^2 w_s}{\partial x^2} + (P_{44}^{'}+2Q_{44}^{'}-2O_{23}+S_{44})\frac{\partial^2 w_s}{\partial y^2} \\
&-U_{33}w_s = -g(z)*q
\end{aligned} \tag{21}$$

6. Solution procedure

The boundary conditions along the edges of the simply supported plate can be obtained as

$$\begin{aligned}
N_1 = M_1 = P_1 = v = w_b = w_s = \frac{\partial w_s}{\partial y} \quad at\ x = 0, a \\
N_2 = M_2 = P_2 = u = w_b = w_s = \frac{\partial w_s}{\partial x} \quad at\ x = 0, b
\end{aligned} \tag{22}$$

To solve this problem, Navier presented the transverse mechanical loads q in the form of a double trigonometric series as

$$q = q_0 \sin(\alpha x)\sin(\beta y) \tag{23}$$

Where q_0 is constant, $\alpha = \pi/a$, $\beta = \pi/b$.

For the analytical solution of Eqs. (18), the Navier method is used under the specified boundary conditions. The displacement functions that satisfy the equations of boundary conditions (22) are selected as the following Fourier series

$$\begin{Bmatrix} u(x,y) \\ v(x,y) \\ w_b(x,y) \\ w_s(x,y) \end{Bmatrix} = \begin{Bmatrix} U\cos(\alpha x)\sin(\beta y) \\ V\sin(\alpha x)\cos(\beta y) \\ W_b\sin(\alpha x)\sin(\beta y) \\ W_s\sin(\alpha x)\sin(\beta y) \end{Bmatrix} \tag{24}$$

By substituting Eqs. (24) and (23) into Eqs. (21), the following equation are obtained

$$[K]\{\Delta\} = \{Q\} \tag{25}$$

Where $\{\Delta\}=\{U, V, W_b, W_s\}^t$ and $\{Q\}=\{0,0,-q_0,-g(h/2)q_0\}^t$ is the symmetric matrix given by

$$[K] = \begin{bmatrix} a_{11} & a_{12} & a_{13} & a_{14} \\ a_{12} & a_{22} & a_{23} & a_{24} \\ a_{13} & a_{23} & a_{33} & a_{34} \\ a_{14} & a_{24} & a_{34} & a_{44} \end{bmatrix} \tag{26}$$

In which

Table 1 Comparison of the dimensionless in-plane longitudinal stress $\overline{\sigma_x}$ and displacement $\overline{w}$ for a FG square plate

p	Theory		$\overline{\sigma}_x$ (1/3)			$\overline{w}$ (0)		
			a/h=4	a/h=10	a/h=100	a/h=4	a/h=10	a/h=100
1	Neves *et al.* (2011)		0.5925	1.4945	14.969	0.6997	0.5845	0.5624
	Ashraf and Zenkour (2013)		0.5944	1.4962	14.552	0.6828	0.5592	0.5459
	Present	Voigt	0.5945	1.4965	14.557	0.6828	0.5592	0.5459
		Reuss	0.4664	1.2068	11.931	0.9950	0.7779	0.7421
		LRVE	0.5311	1.3566	13.323	0.8674	0.6944	0.6685
		Tamura	0.5252	1.3419	13.179	0.8634	0.6897	0.6637
		Mori-Tanaka	0.5000	1.2844	12.652	0.9188	0.7272	0.6971
4	Neves *et al.* (2011)		0.4404	1.1783	11.932	1.1178	0.8750	0.8286
	Ashraf and Zenkour (2013)		0.4321	1.1410	11.388	1.1001	0.8404	0.7933
	Present	Voigt	0.4324	1.1416	11.395	1.1000	0.8404	0.7933
		Reuss	0.3552	0.9399	9.3895	1.3748	1.0285	0.9667
		LRVE	0.3601	0.9632	9.6600	1.2675	0.9424	0.8827
		Tamura	0.3690	0.9823	9.8338	1.2641	0.9449	0.8868
		Mori-Tanaka	0.3604	0.9577	9.5816	1.3112	0.9793	0.9192
10	Neves *et al.* (2011)		0.3227	1.1783	11.932	1.3490	0.8750	0.8286
	Ashraf and Zenkour (2013)		0.3154	0.8530	8.5853	1.3391	0.9806	0.9140
	Present	Voigt	0.3156	0.8535	8.5914	1.3391	0.9806	0.9139
		Reuss	0.3525	0.9191	9.1335	1.5789	1.1972	1.1337
		LRVE	0.3133	0.8297	8.2911	1.4849	1.1075	1.0407
		Tamura	0.3253	0.8599	8.5886	1.4832	1.1075	1.0412
		Mori-Tanaka	0.3355	0.8814	8.7836	1.5244	1.1458	1.0805

$$
\begin{aligned}
a_{11} &= -\left(\alpha^2 A_{11} + \beta^2 A_{66}\right) \\
a_{12} &= -\alpha\beta\left(A_{12} + A_{66}\right) \\
a_{13} &= \alpha^3 B_{11} + \alpha\beta^2\left(B_{12} + 2B_{66}\right) \\
a_{14} &= -\alpha^3 C_{11} - \alpha\beta^2\left(C_{12} + 2C_{66}\right) + \alpha F_{13} \\
a_{22} &= -\left(\beta^2 A_{22} + \alpha^2 A_{66}\right) \\
a_{23} &= \beta^3 B_{22} + \alpha^2\beta\left(B_{12} + 2B_{66}\right) \\
a_{24} &= -\beta^3 C_{22} - \alpha^2\beta\left(C_{12} + 2C_{66}\right) + \beta F_{23} \\
a_{33} &= -\alpha^4 G_{11} - \beta^4 G_{22} - 2\alpha^2\beta^2\left(G_{12} + 2G_{66}\right) \\
a_{34} &= \alpha^4 H_{11} + \beta^4 H_{22} + 2\alpha^2\beta^2\left(H_{12} + 2H_{66}\right) - \alpha^2 K'_{13} - \beta^2 K'_{23} \\
a_{44} &= -\alpha^4 L_{11} - \beta^4 L_{22} - 2\alpha^2\beta^2\left(L_{12} + 2L_{66}\right) - \beta^2\left(Q'_{44} + P'_{44}\right) \\
&\quad - \alpha^2\left(Q'_{55} + P'_{55}\right) - \beta^2\left(S_{44} + Q'_{44}\right) - \alpha^2\left(S_{55} + Q'_{55}\right) \\
&\quad + 2\alpha^2 O_{13} + 2\beta^2 O_{23} - U_{33}
\end{aligned}
\tag{27}
$$

7. Numerical results and discussion

In the present section, the effect of micromechanical models on bending analysis of FG plates using a new quasi-3D shear deformation theory is presented for investigation. In order to verify the accuracy of the present analysis, the results of this study were verified by comparing them with the various existing plate theories. The material properties used in the present study are:

- Metal in bottom surface (Aluminium, Al): $E_M = 70 \times 10^9$ N/m2; $\nu = 0.3$; $\rho_M = 2702$ kg/m3.
- Ceramic in top surface (Alumina, Al2O3): $E_C = 380 \times 10^9$; N/m2; $\nu = 0.3$; $\rho_C = 3800$ kg/m3.

For simplicity, the following non-dimensional parameters are used in the numerical examples

$$
\begin{aligned}
&\bar{w} = \frac{100 E_c h^3}{q_0 a^4} w\left(\frac{a}{2}, \frac{b}{2}, \bar{z}\right), \quad \bar{\sigma}_x = \frac{h}{q_0 a}\sigma_x\left(\frac{a}{2}, \frac{b}{2}, \bar{z}\right) \\
&\bar{\sigma}_y = \frac{h}{q_0 a}\sigma_y\left(\frac{a}{2}, \frac{b}{2}, \bar{z}\right), \quad \bar{\sigma}_z = \frac{1}{q_0}\sigma_z\left(\frac{a}{2}, \frac{b}{2}, \bar{z}\right), \\
&\bar{\tau}_{yz} = \frac{h}{q_0 a}\tau_{yz}\left(\frac{a}{2}, 0, \bar{z}\right), \quad \overline{\tau_{xz}} = \frac{h}{q_0 a}\tau_{xz}\left(0, \frac{b}{2}, \bar{z}\right), \\
&\bar{\tau}_{xy} = \frac{h}{q_0 a}\tau_{xy}\left(0, 0, \bar{z}\right), \quad \bar{z} = \frac{z}{h}
\end{aligned}
\tag{28}
$$

Where

$\overline{\sigma_x}$ is in- plane longitudinal stress

Table 2 Comparison of the dimensionless stresses and displacements of a FG square plate (a=10h)

p	Theory		$\bar{w}$ (0)	$\bar{\sigma}_x$ (1/2)	$\bar{\sigma}_y$ (1/3)	$\bar{\tau}_{yz}$ (1/6)	$\bar{\tau}_{xz}$ (0)	$\bar{\tau}_{xy}$ (-1/3)
0	Ashraf and zenkour (2013)		0.2881	2.0645	1.3456	0.2963	0.3335	0.6689
	Present	Voigt	0.2881	2.0635	1.3458	0.2963	0.3333	0.6689
		Reuss	0.2881	2.0635	1.3458	0.2963	0.3333	0.6689
		LRVE	0.2881	2.0635	1.3458	0.2963	0.3333	0.6689
		Tamura	0.2881	2.0635	1.3458	0.2963	0.3333	0.6689
		Mori-Tanaka	0.2881	2.0635	1.3458	0.2963	0.3333	0.6689
1	Ashraf and zenkour (2013)		0.5592	3.1756	1.4962	0.3644	0.3335	0.5486
	Present	Voigt	0.5592	3.1738	1.4965	0.3643	0.3333	0.5486
		Reuss	0.7779	4.0621	1.2068	0.3064	0.2655	0.5235
		LRVE	0.6944	3.6551	1.3567	0.3399	0.2852	0.5107
		Tamura	0.6897	3.6639	1.3419	0.3351	0.2869	0.5207
		Mori-Tanaka	0.7272	3.8231	1.2844	0.3229	0.2763	0.5205
2	Ashraf and zenkour (2013)		0.7158	3.6833	1.3775	0.3502	0.2797	0.4853
	Present	Voigt	0.7158	3.6812	1.3780	0.3501	0.2796	0.4853
		Reuss	0.9081	4.7183	1.0466	0.2726	0.2456	0.5299
		LRVE	0.8301	4.1561	1.1558	0.2943	0.2397	0.5096
		Tamura	0.8285	4.2008	1.1577	0.2967	0.2477	0.5114
		Mori-Tanaka	0.8616	4.4012	1.1050	0.2848	0.2452	0.5193
5	Ashraf and zenkour (2013)		0.8729	4.2607	1.0651	0.2607	0.2110	0.5213
	Present	Voigt	0.8729	4.2580	1.0657	0.2606	0.2108	0.5213
		Reuss	1.0683	5.9644	0.9216	0.2454	0.2529	0.5626
		LRVE	0.9793	5.1145	0.9142	0.2349	0.2309	0.5444
		Tamura	0.9818	5.1571	0.9390	0.2425	0.2337	0.5449
		Mori-Tanaka	1.0176	5.4838	0.9252	0.2428	0.2417	0.5523
10	Ashraf and zenkour (2013)		0.9806	5.0901	0.8530	0.2173	0.2281	0.5442
	Present	Voigt	0.9806	5.0870	0.8535	0.2172	0.2279	0.5442
		Reuss	1.1972	7.2434	0.9191	0.2502	0.2777	0.5879
		LRVE	1.1075	6.3247	0.8297	0.2349	0.2598	0.5687
		Tamura	1.1075	6.3250	0.8599	0.2365	0.2593	0.5693
		Mori-Tanaka	1.1458	6.7133	0.8814	0.2424	0.2675	0.5772
Metal	Ashraf and zenkour (2013)		1.5642	2.0645	1.3456	0.2963	0.3335	0.6689
	Present	Voigt	1.5642	2.0635	1.3458	0.2963	0.3333	0.6689
		Reuss	1.5642	2.0635	1.3458	0.2963	0.3333	0.6689
		LRVE	1.5642	2.0635	1.3458	0.2963	0.3333	0.6689
		Tamura	1.5642	2.0635	1.3458	0.2963	0.3333	0.6689
		Mori-Tanaka	1.5642	2.0635	1.3458	0.2963	0.3333	0.6689

$\overline{\sigma_y}$ is the in- plane normal stress,

$\overline{\sigma_z}$ is the transverse normal stress,

$\bar{w}$ is the transverse displacement,

$\bar{\tau}_{xz}$ is the transverse shear stress.

7.1 Comparison between different micromechanical models

A comparison between the Young's modulus values calculated from the various micromechanical models is

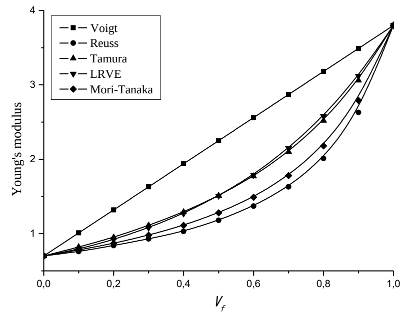

Fig. 2 Effective Young's modulus as function of volume fraction of ceramic for several micromechanical models

shown in Fig. 2. The estimated results are depicted as a function of volume fraction of inclusions (ceramic). The first observation emerging from this figure is that the models of Voigt and Reuss give the values max and min of the Young's modulus respectively. The second observation is that the models of Tamura (q=-100GPa) and LRVE give practically the same result in term of Young's modulus and this whatever the value of the volume fraction. These Young modulus values are slightly higher than those calculated by the Mori-Tanaka model.

7.2 Comparison studies

Firstly, the example is performed in table 1 for a square plate with power law index p=1,4 and 10. Effective Young's modulus is calculated using the aforementioned five micromechanical models. The obtained results are compared with quasi-3-dimensional (3D) theory developed by Ashraf and Zenkour (2013) and theory Neves *et al.* (2011) theory where εz=0.

From this table two observations can be made.

First, the results obtained from the present quasi 3D theory for the Voigt model are very close to those of Ashraf and Zenkour (2013) and this for the stress or the deflection. While a slight difference is observed after comparison with the results of the theory developed by Neves *et al.* (2011). This is due to the fact that the latter does not take into account the normal deformation (εz=0). Secondly, the results from the present method and calculated with the four other models, namely LRVE, Tamura, Mori-Tanaka and Reuss, are slightly different. This can be explained by the way who the Young's modulus is calculated. It should be noted that a comparison between the different values of the Young's modulus calculated by the different models was commented on in the previous paragraph.

In Table 2, a second comparison is made between the results of the present quasi 3D theory with the various micromechanical models and those of Ashraf and Zenkour (2013). The results are given in terms of deflection and the various constraints. Here again we note the same observation that the results are very close for the model of Voigt and a slight difference is noticed compared to the others.

7.3 Parametric studies

In the present paragraph some results and considerations about the effect of the micromechanical models on the bending problem of functionally plates are presented. The analysis has been carried out by means of numerical procedures illustrated above.

The influence of the volume fraction index "p" on the variation of the out-of-plane displacement $\bar{w}$ through the thickness direction is showed in Fig. 3. It should be noted that the Voigt model was used in this example. It can be seen from Figure 3 that the transverse displacement $\bar{w}$ of metal plates is larger than the corresponding one of ceramic plates and in general, the transverse displacement increases as the volume fraction index "p" increases.

In Fig. 4, the variations of the out-of-plane displacement

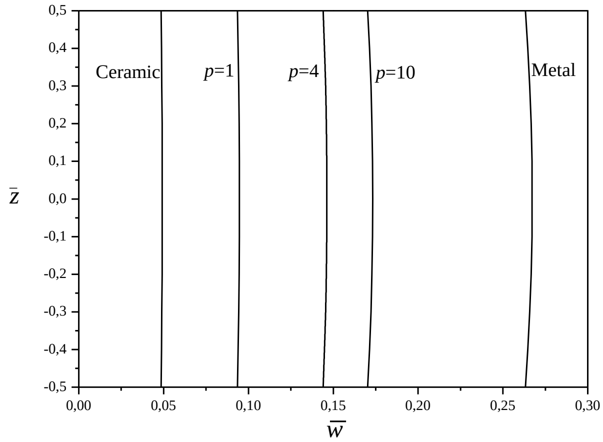

Fig. 3 The transverse displacement $\bar{w}$ through the thickness of FG plates (a/h=10, a=$2b$). Voigt model

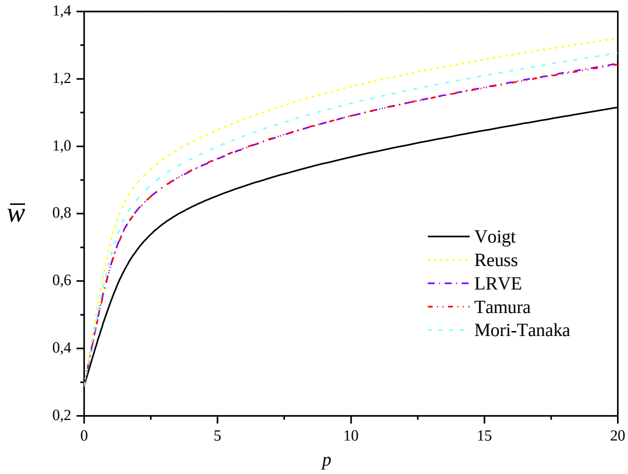

Fig. 4 The transverse displacement $\bar{w}$ versus the power law index "p" of FG square plates for different micromechanical models (a/h=10)

$\bar{w}$ through the thickness direction of FG plate with the power law index "p" are given for different micromechanical models. It is seen from the figure that the increase of the power law index "p" produces an increase in the values of the displacement and this whatever the model used.

In addition, the Reuss model has the highest displacement values compared to other models. While that of Voigt has the lowest values. The LRVE and Tamura models have the practically same results.

Relative Percentage difference of the out-of-plane displacement $\bar{w}$ between micromechanical models versus power law index "p" is shown in Fig. 5.

The discrepancy between the estimated out-of-plane displacement $\bar{w}$ of FGMs plate by Reuss, LRVE, Tamura and other micromechanical models depends considerably on the power law index "p".

The discrepancy between the Reuss model and other micro- mechanical models for the estimated value of the out-of-plane displacement reaches a maximum of 10% between Reuss-LRVE and Reuss-Tamura and it is 6%

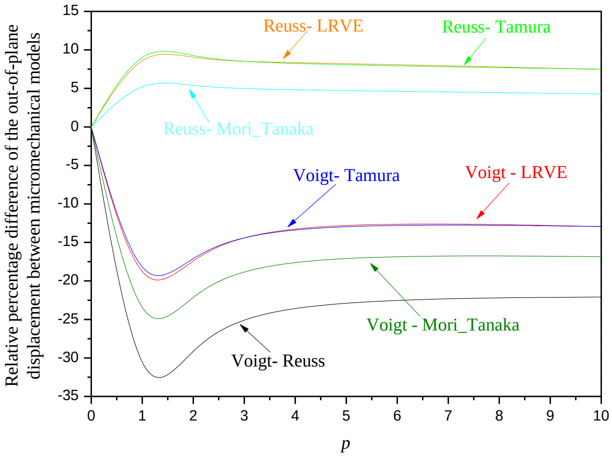

Fig. 5 Relative percentage difference between the micromechanical models of the transverse displacement $\bar{w}$ of FG square plates (a/h=10)

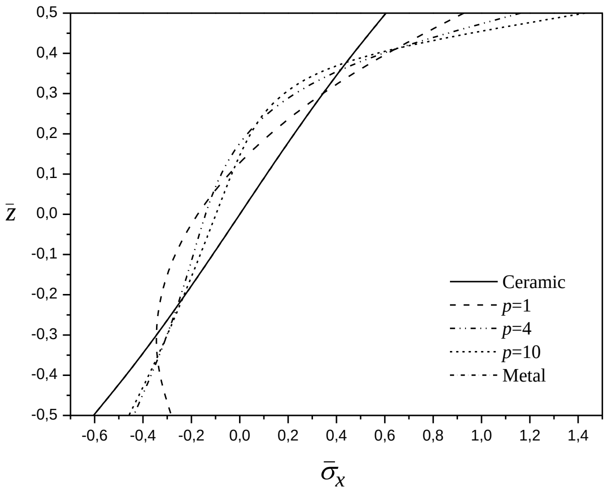

Fig. 6 The in-plane longitudinal stress $\bar{\sigma}_x$ through the thickness of a FG rectangular plate (a/h=10) -Voigt model-

between Reuss-Mori-Tanaka.

The second comparison shown in this figure is the discrepancy between the values of the out-of-plane displacement between the Voigt model and other micromechanical models. The difference is insignificant between Voigt and Tamura and it reached a maximum of 33% between Voigt and other models. Therefore, the necessity of the proper micromechanical modeling of FGMs is evident to accurately estimate the fundamental frequency.

In Fig. 6, the in-plane longitudinal stress $\bar{\sigma}x$ through the thickness is tensile at the top surface and compressive at the bottom surface. The homogeneous ceramic plate p=0 or metal plate p=∞ yields the maximum compressive stresses at the bottom surface and the minimum tensile stresses at the top surface of the FG plates.

In Fig. 7, we present the variation of the in-plane longitudinal stress $\bar{\sigma}x$ through the thickness for different micromechanical models. From this figure, it can be seen that all models give practically the same results in terms of axial stress except that of Voigt, which gives minimum

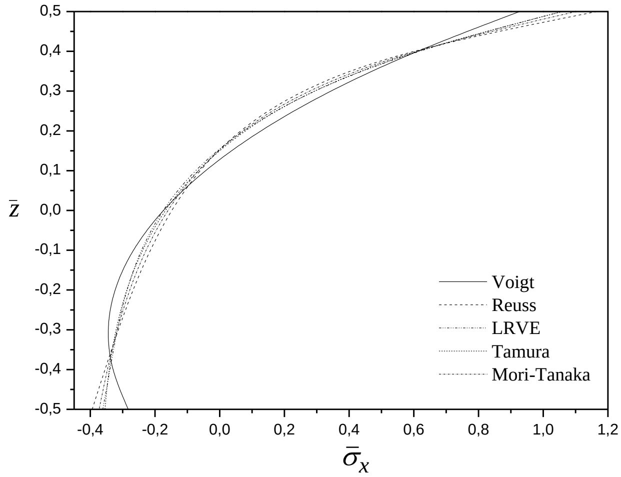

Fig. 7 The in-plane longitudinal stress $\bar{\sigma}_x$ through the thickness of a FG rectangular plate for different micromechanical models (a/h=10, a=2b, p=1)

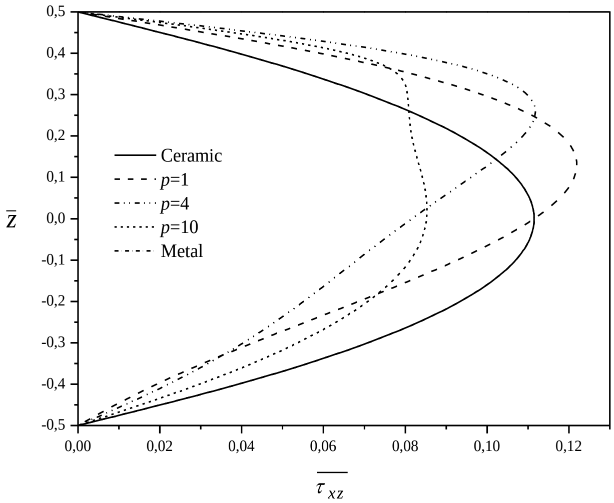

Fig. 8 The transverse shear stress $\bar{\tau}_{xz}$ through the thickness of a FG rectangular plate (a/h=10, a=2b) -Voigt model-

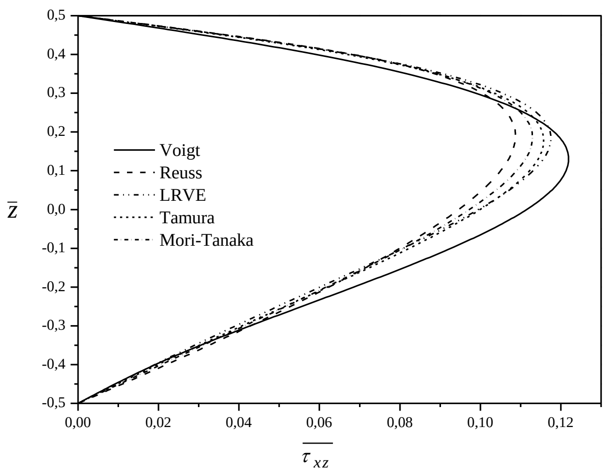

Fig. 9 The transverse shear stress $\bar{\tau}_{xz}$ through the thickness of a FG rectangular plate for different micromechanical models (a/h=10, a=2b, p=1)

tensile stresses at the top, and maximum compressive stresses at the bottom surface.

In Fig. 8, we have plotted the variation of the transverse shear stress $\bar{\tau}_{xz}$ through-the-thickness of a FG rectangular plate using the Voigt model.

The through-the-thickness distributions of the transverse shear stresses are not parabolic in the case of non-homogenous plate as in the case of homogeneous plates (ceramic or metal).

It can be observed that increasing the power-law index p leads to a reduction of the transverse shear stress in the skin of the plate. Also, it is found that the homogeneous plates that are either metal or ceramic give the same transverse shear stress

The effect of the micromechanical models on the variation of the transverse shear stress $\bar{\tau}_{xz}$ across the thickness is shown in Fig. 9. The Voigt model is the one, which gives the highest stresses compared with the others where the difference between the max stresses is minimal.

8. Conclusions

In this paper, we have developed a new refined quasi-three-dimensional (3D) shear deformation theory for the solutions of static bending of FG plate.

The theory accounts for parabolic distribution of the transverse shear strains and satisfies the zero traction boundary conditions on the surfaces of the functionally graded plate without using shear correction factors. The highlight of this theory is that, in addition to including the thickness stretching effect, the displacement field is modeled with only 4 unknowns, which is even less than the other shear and normal deformation theories where we find five, six or more variables. Different micromechanical models were used to determine the effective properties of the FG plates. The Navier method is used for the analytical solutions of the FG plate with simply supported boundary conditions.

The results obtained using this new theory, are in a good agreement with reference solutions available in literature.
Among the results that could be determined after the parametric study:

- The discrepancy between the estimated out-of-plane displacement $\bar{w}$ of FGMs plate by Reuss, LRVE, Tamura and other micromechanical models depends considerably on the power law index “p”.
- All micromechanical models give practically the same results in terms of axial stress except that of Voigt which gives minimum tensile stresses at the top and maximum compressive stresses at the bottom surface.
- For the transverse shear stress the Voigt model is the one which gives the highest stresses compared with the others where the difference between the max stresses is minimal.

From these results and comparisons between different micromechanical models, it has been found significant differences between some models. This proves the need for a proper micromechanical modeling of FGMs to accurately estimate the deflection and stress.

Finally, it can be said that the proposed quasi 3D shear deformation theory can be extended to study thermal behavior on the basis of works of Bouderba *et al.* (2016), Bousahla *et al.* (2016), Bousahla *et al.* (2016), Chikh *et al.* (2017) and Khetir *et al.* (2017).

References

Abdelaziz, H.H., Atmane, H.A., Mechab, I., Boumia, L., Tounsi, A., Adda Bedia, E.A. (2011), “Static analysis of functionally graded sandwich plates using an efficient and simple refined theory”, *Chin. J. Aeronaut.*, **24**(4), 434-448.

Aboudi, J., Pindera, M.J. and Arnold, S.M. (1996), “Thermoelastic theory for the response of materials graded in two directions”, *Int. J. Sol. Struct.*, **33**(7), 931-966.

Aboudi, J., Pindera, M.J. and Arnold, S.M. (1999), “Higher order theory for functionally graded materials”, *Compos. B*, **30**(8), 777-832.

Abualnour, M., Houari, M.S.A., Tounsi, A. and Mahmoud, S.R. (2017), “A novel quasi-3D trigonometric plate theory for free vibration analysis of advanced composite plates”, *Compos. Struct.*, **184**, 688-697.

Ait Amar Meziane, M., Abelazziz H.H. and Tounsi, A. (2014), “An efficient and simple refined theory for buckling and free vibration of exponentially graded sandwich plates under various boundary conditions”, *J. Sandw. Struct. Mater.*, **16**(3), 293-318.

Ait Atmane, H., Tounsi, A., Bernard, F. and Mahmoud, S.R. (2015), “A computational shear displacement model for vibrational analysis of functionally graded beams with porosities”, *Steel Compos. Struct.*, **19**(2), 369-384.

Akavci, S.S. (2014), “An efficient shear deformation theory for free vibration of functionally graded thick rectangular plates on elastic foundation”, *Compos. Struct.*, **108**, 667-676.

Akbarzadeh, A.H., Abedini, A. and Chen, Z.T. (2015), “Effect of micromechanical models on structural responses of functionally graded plates”, *Compos. Struct.*, **119**, 598-609.

Ashraf, M. and Zenkour. (2013), “A simple four unknown refined theory for bending analysis of functionally graded plates”, *Appl. Math. Mod.*, **37**(20-21), 9041-9051.

Belabed, Z., Houari, M.S.A, Tounsi, A., Mahmoud, S.R. and Anwar, Bég. O. (2014), “An efficient and simple higher order shear and normal deformation theory for functionally graded material (FGM) plates”, *Compos. Part B*, **60**, 274-283.

Bellifa, H. Benrahou, K.H. and Tounsi, A. (2016), “Bending and free vibration analysis of functionally graded plates using a simple shear deformation theory and the concept the neutral surface position”, *Braz. Soc. Mech. Sci. Eng.*, **38**(1), 265-275.

Bellifa, H., Bakora, A., Tounsi, A., Bousahla, A.A. and Mahmoud, S.R. (2017), “An efficient and simple four variable refined plate theory for buckling analysis of functionally graded plates”, *Steel Compos. Struct.*, **25**(3), 257-270.

Bellifa, H., Benrahou, K.H., Hadji, L., Houari, M.S.A. and Tounsi, A. (2016), “Bending and free vibration analysis of functionally graded plates using a simple shear deformation theory and the concept the neutral surface position”, *J. Braz. Soc. Mech. Sci. Eng.*, **38**(1), 265-275.

Benachour, A., Daouadji, H.T., Ait Atmane, H., Tounsi, A. and Meftah, S.A. (2011), “A four variable refined plate theory for free vibrations of functionally graded plates with arbitrary gradient”, *Compos. Part B-Eng.*, **42**(6), 1386-1394.

Benchohra, M., Driz, H., Bakora, A., Tounsi, A., Adda Bedia, E. A. and Mahmoud, S.R. (2018), “A new quasi-3D sinusoidal shear deformation theory for functionally graded plates”, *Struct. Eng. Mech.*, **65**(1), 19-31.

Bennoun, M., Houari, M.S.A. and Tounsi, A. (2016), “A novel five variable refined plate theory for vibration analysis of functionally graded sandwich plates", *Mech. Adv. Mater. Struct.*, **23**(4), 423-431.

Benveniste, Y. (1987), "A new approach to the application of Mori-Tanaka's theory in composite materials", *Mech. Mat.*, **6**(2), 147-157.

Bessaim, A., Houari, M.S.A., Tounsi, A., Mahmoud, S.R. and Adda Bedia, E.A. (2013), "A new higher-order shear and normal deformation theory for the static and free vibration analysis of sandwich plates with functionally graded isotropic face sheets", *Sandw. Struct. Mater.*, **15**(6), 671-703.

Bouderba, B, Houari, MSA. And Tounsi, A. (2013), "Thermomechanical bending response of FGM thick plates resting on Winkler-Pasternak elastic foundations", *Steel Compos. Struct.*, **14**(1), 85-104.

Bouderba, B., Houari, M.S.A. and Tounsi, A. and Mahmoud, S.R. (2016), "Thermal stability of functionally graded sandwich plates using a simple shear deformation theory", *Struct. Eng. Mech.*, **58**(3), 397-422.

Boukhari, A., Ait Atmane, H., Tounsi, A., Adda Bedia, E.A. and Mahmoud, S.R. (2016), "An efficient shear deformation theory for wave propagation of functionally graded material plates", *Struct. Eng. Mech.*, **57**(5), 837-859.

Bourada, M., Kaci, A., Houari, M.S.A. and Tounsi, A. (2015), "A new simple shear and normal deformations theory for functionally graded beams", *Compos. Struct.*, **18**(2), 409-423.

Bourada, M., Tounsi, A., Houari, M.S.A. and Adda Bedia, E.A. (2012), "A new four-variable refined plate theory for thermal buckling analysis of functionally graded sandwich plates", *J. Sandw. Struct. Mater.*, **14**(1), 5-33.

Bousahla, A.A., Benyoucef, S., Tounsi, A. and Mahmoud, S.R. (2016), "On thermal stability of plates with functionally graded coefficient of thermal expansion", *Struct. Eng. Mech.*, **60**(2), 313-335.

Bousahla, A.A., Houari, M.S.A., Tounsi, A. and Adda Bedia, E.A. (2014), "A novel higher order shear and normal deformation theory based on neutral surface position for bending analysis of advanced composite plates", *Int. J. Comput. Meth.*, **11**(6), 1350082.

Brischetto, S. (2014), "An exact 3D solution for free vibrations of multilayered cross-ply composite and sandwich plates and shells", *Int. J. Appl. Mech.*, **6**(6), 1450076.

Chi, S.H. and Chung, Y.L. (2006), "Mechanical behavior of functionally graded material plates under transverse load-part II: Numerical results", *Int. J. Sol. Struct.*, **43**(13), 3675-3691.

Chi, S. and Chung, Y. (2006a), "Mechanical behavior of functionally graded material plates under transverse load-part I: Analysis", *Int. J. Sol. Struct.*, **43**(13), 3657-3674.

Chi, S. and Chung, Y. (2006b), "Mechanical behavior of functionally graded material plates under transverse load-part II: numerical results", *Int. J. Sol. Struct.*, **43**(13), 3675-3691.

Chikh, A., Tounsi, A., Hebali, H. and Mahmoud, S.R. (2017), "Thermal buckling analysis of cross-ply laminated plates using a simplified HSDT", *Smart Struct. Syst.*, **19**(3), 289-297.

Draiche, K., Tounsi, A. and Mahmoud, S.R. (2016), "A refined theory with stretching effect for the flexure analysis of laminated composite plates", *Geo. Mech. Int. J.*, **11**(5), 671-690.

Farzam-Rad, S.A., Hassani, B. and Karamodin, A. (2016), "Isogeometric analysis of functionally graded plates using a new quasi-3D shear deformation theory based on physical neutral surface", *Compos. Part B Eng.*, **108**, 174-189.

Fekrar, A., Houari, M.S.A., Tounsi, A. and Mahmoud, S.R. (2014), "A new five-unknown refined theory based on neutral surface position for bending analysis of exponential graded plates", *Meccan.*, **49**(4), 795-810.

Gasik, M. (1995), "Scand. Ch226", *Acta Polytech*, **72**.

Gasik, M.M. (1998), "Micromechanical modeling of functionally graded materials", *Comput. Mater. Sci.*, **13**, 42-55.

Gupta, A. and Talha, M. (2017), "Nonlinear flexural and vibration response of geometrically imperfect gradient plates using hyperbolic higher-order shear and normal deformation theory", *Compos. Part B Eng.*, **123**, 241-261.

Hadji, L., Atmane, H.A., Tounsi, A., Mechab, I. and Adda Bedia, E.A. (2011), "Free vibration of functionally graded sandwich plates using four variable refined plate theory", *Appl. Math. Mech.*, **32**(7), 925-942.

Hebali, H., Tounsi, A., Houari, M.S.A, Bessaim, A. and Adda Bedia, E.A. (2014), "New quasi-3D hyperbolic shear deformation theory for the static and free vibration analysis of functionally graded plates", *J. Eng. Mech.*, **140**(2), 374-383.

Houari, M.S.A., Benyoucef, S., Mechab, I., Tounsi, A. and Adda Bedia, E.A. (2011), "Two variable refined plate theory for thermoelastic bending analysis of functionally graded sandwich plates", *J. Therm. Stress.*, **34**(4), 315-334.

Houari, M.S.A., Tounsi, A., Bessaim, A. and Mahmoud, S.R. (2016), "A new simple three-unknown sinusoidal shear deformation theory for functionally graded plates", *Steel Compos. Struct.*, **22**(2), 257-276.

Huu-Tai, T., Thuc, P.V., Tinh, Q.B. and Nguyen, T.K. (2014), "A quasi-3D hyperbolic shear deformation theory for functionally graded plates", *Acta Mech.*, **225**(3), 951-964.

Jaesang, Y. and Addis, K. (2014), "Modeling functionally graded materials containing multiple heterogeneities", *Acta Mech.*, **225**(7), 1931-1943.

Jha, D.K., Kant, T. and Singh, R.K. (2013), "Critical review of recent research on functionally graded plates", *Compos. Struct.*, **96**, 833-849.

Ju, J. and Chen, T.M. (1994), "Micromechanics and effective moduli of elastic composites containing randomly dispersed ellipsoidal inhomogeneities", *Acta Mech.*, **103**(1-4), 103-121.

Khetir, H., Bachir Bouiadjra, M., Houari, M.S.A., Tounsi, A. and Mahmoud, S.R. (2017), "A new nonlocal trigonometric shear deformation theory for thermal buckling analysis of embedded nanosize FG plates", *Struct. Eng. Mech.*, **64**(4), 391-402.

Koizumi, M. (1993), "The concept of FGM", *Ceram. Trans. Funct. Grad. Mater.*, **34**, 3-10.

Merazi, M., Hadji, L., Daouadji, T. H., Tounsi, A. and Adda Bedia, E.A. (2015), "A new hyperbolic shear deformation plate theory for static analysis of FGM plate based on neutral surface position", *Geomech. Eng.*, **8**(3), 305-321.

Merdaci, S., Tounsi, A., Houari, M.S.A., Mechab, I., Hebali, H. and Benyoucef, S. (2011), "Two new refined shear displacement models for functionally graded sandwich plates", *Arch. Appl. Mech.*, **81**(11), 1507-1522.

Mishnaevsky, J.L. (2007), *Computational Mesomechanics of Composites*, John Wiley & Sons, U.K.

Mori, T. and Tanaka, K. (1973), "Average stress in matrix and average elastic energy of materials with misfitting inclusions", *Acta Metall.*, **21**(5), 571-574.

Neves, A.M.A., Ferreiraa, A.J.M., Carrerac, E., Roqueb, C.M.C., Cinefrac, M., Jorgea, R.M.N. and Soares, C.M.M. (2011), "Bending of FGM plates by a sinusoidal plate formulation and collocation with radial basis functions", *Mech. Res. Commun.*, **38**(5), 368-371.

Neves, A.M.A., Ferreira, A.J.M., Carrera, E., Cinefra, M., Roque, C.M.C. and Jorge, R.M.N. (2012), "A quasi-3D hyperbolic shear deformation theory for the static and free vibration analysis of functionally graded plates", *Compos. Struct.*, **94**(5), 1814-1825.

Ostoja-Starzewski, M., Jasiuk, I., Wang, W. and Alzebdeh, K. (1996), "Composite with functionally graded interphases: Mesocontinuum concept and effective transverse conductivity", *Acta Metall.*, **44**(5), 2057-2066.

Ould Larbi, L., Kaci, A., Houari, M.S.A. and Tounsi, A. (2013), "An efficient shear deformation beam theory based on neutral surface position for bending and free vibration of functionally graded beams", *Mech. Bas. Des. Struct. Mach.*, **41**(4), 421-433.

Ould Youcef, D., Kaci, A., Benzair, A., Bousahla, A.A. and Tounsi, A. (2018), "Dynamic analysis of nanoscale beams including surface stress effects", *Smart Struct. Syst.*, **21**(1), 65-74.

Pindera, M.J., Aboudi, J. and Arnold, S.M. (2002), "Analysis of spallation mechanism in thermal barrier coatings with graded bond coats using the higher-order theory of FGM", *Eng. Fract. Mech.*, **69**(14-16), 1587-1606.

Reddy, J.N. (2000), "Analysis of functionally graded plates", *Int. J. Numer. Meth. Eng.*, **47**(1-3), 663-684.

Shen, H.S. and Wang, Z.X. (2012), "Assessment of Voigt and Mori–Tanaka models for vibration analysis of functionally graded plates", *Compos. Struct.*, **94**(7), 2197-2208.

Taibi, F.Z., Benyoucef, S., Tounsi, A., Bachir Bouiadjra, R., Adda Bedia, E.A. and Mahmoud, S.R. (2015), "A simple shear deformation theory for thermo-mechanical behaviour of functionally graded sandwich plates on elastic foundations", *J. Sandw. Struct. Mater.*, **17**(2), 99-129.

Talha, M. and Singh, B.N. (2010), "Static response and free vibration analysis of FGM plates using higher order shear deformation theory", *Appl. Math. Model.*, **34**(12), 3991-4011.

Talha, M. and Singh, B.N. (2011), "Thermo-mechanical induced vibration characteristics of shear deformable functionally graded ceramic-metal plates using finite element method", *Proc. Inst. Mech. Eng. Part C J. Mech. Eng. Sci.*, **225**(1), 50-65.

Tounsi, A., Houari, M.S.A. and Bessaim, A. (2016), "A new 3-unknowns non-polynomial plate theory for buckling and vibration of functionally graded sandwich plate", *Struct. Eng. Mech.*, **60**(4), 547-565.

Tounsi, A., Houari, M.S.A. Benyoucef, S. and Adda Bedia, E.A. (2013), "A refined trigonometric shear deformation theory for thermoelastic bending of functionally graded sandwich plates", *Aerosp. Sci. Technol.*, **24**(1), 209-220.

Yaghoobi, H. and Torabi, M. (2013), "Post-buckling and nonlinear free vibration analysis of geometrically imperfect functionally graded beams resting on nonlinear elastic foundation", *Appl. Math. Model.*, **37**(18-19), 8324-8340.

Yin, H.M., Paulino, G.H., Buttlar, W.G. and Sun, L.Z. (2007), "Micromechanics-based thermoelastic model for functionally graded particulate materials with particle interactions", *J. Mech. Phys. Sol.*, **55**(1), 132-160.

Yin, H.M., Sun, L.Z. and Paulino, G.H. (2004), "Micromechanics-based elastic model for functionally graded particulate materials with particle interactions", *Acta Mater.*, **52**(12), 3535-3543.

Zimmerman, R.W. (1994), "Behavior of the Poisson ratio of a two-phase composite material in the high-concentration limit", *Appl. Mech. Rev.*, **47**(1), 38-44.

Zuiker, J.R. (1995), "Functionally graded materials-choice of micromechanics model and limitations in property variation", *Compos. Eng.*, **5**(7), 807-819.

CC